

Multiple quantum phase transitions of plutonium compounds

Munehisa Matsumoto,¹ Quan Yin,^{1,2} Junya Otsuki,³ and Sergey Yu. Savrasov¹

¹*Department of Physics, University of California, Davis, California 95616, USA*

²*Department of Physics and Astronomy, Rutgers University, Piscataway, New Jersey 08854, USA*

³*Department of Physics, Tohoku University, Sendai 980-8578, Japan*

(Received 5 July 2011; published 22 July 2011)

We show by quantum Monte Carlo simulations of realistic Kondo lattice models derived from electronic-structure calculations that multiple quantum critical points can be realized in plutonium-based materials. We place representative systems, including PuCoGa₅, on a realistic Doniach phase diagram and identify the regions where the magnetically mediated superconductivity could occur. The solution of an inverse problem to restore the quasiparticle renormalization factor for f electrons is shown to be sufficiently good to predict the trends among Sommerfeld coefficients and magnetism. A suggestion on the possible experimental verification for this scenario is given for PuAs.

DOI: [10.1103/PhysRevB.84.041105](https://doi.org/10.1103/PhysRevB.84.041105)

PACS number(s): 71.27.+a, 75.30.Kz, 75.40.Mg

Motivation. Discovery of unconventional superconductivity in PuCoGa₅ (Refs. 1 and 2) opened a new arena for studying strongly correlated materials. It has the highest superconducting transition temperature $T_c = 18.5$ K among f -electron-based materials, and it has been discussed to reside somewhere in between the cerium-based heavy-fermion (HF) superconductors and high- T_c cuprates, where the latter still challenges theoretical control from first principles.

In the present work we make predictions on the magnetism and HF behavior of several Pu compounds, including Pu-115's, where the mechanism of possible magnetically mediated superconductivity is discussed to be more complicated than their cerium counterparts.³ Furthermore, with experimental challenges such as the self-heating of samples due to the radiative nature of Pu nuclei, a computational guide should be of help regarding the determination of the linear coefficient of electronic heat capacity, the so-called Sommerfeld coefficient γ . Our computational method is based on a recently developed scheme for realistic Kondo lattice simulations,^{4,5} which enabled us to predict the location of the magnetic quantum critical point (QCP)⁶ from electronic structure calculations⁷ for HF materials.

Our main results are shown in Fig. 1 in the format of a Doniach phase diagram⁸ plotted with realistic settings for the target materials. A striking double-dome structure is seen both in the magnetic Doniach phase diagram of PuCoGa₅ plotted on the (J_K, T_N) plane and an analogous plot on the (J_K, γ) plane, where J_K is the Kondo coupling and T_N is the Neel temperature. For Pu-115's there are at least two antiferromagnetic phases with at least three QCP's. We see that Pu-115's are, indeed, separated from the first, i.e., lowest-energy, magnetic QCP, which is consistent with the situation discussed in Ref. 3. However, we find that the second and third QCP's are encountered on the J_K axis, and the realistic point for Pu-115 is actually in proximity to the latter. Those quantum phase transitions are generally driven by the competition between the Kondo-screening energy scale and the magnetic-ordering energy scale.⁸ The higher-energy QCP's are understood as an outcome of the strong-coupling nature⁹ of the realistic Kondo lattice where, in our simulations, a particular behavior for quasiparticle residue of conduction electron exhibits a dip around the first QCP, letting f spins show up again.

Methods. The electronic structure calculation based on local density approximation (LDA) combined with dynamical mean-field theory (DMFT) (LDA + DMFT) has been successful in addressing interesting properties of strongly correlated materials.⁷ What motivates us for the Kondo-lattice model (KLM) description of HF materials is that efficient and exact quantum Monte Carlo (QMC) simulations in the low-temperature region are possible,¹⁰ typically around $O(10)$ K and down to $O(1)$ K. This advantage is due to having only f spins and eliminating the f electron charge degrees of freedom via Schrieffer-Wolff transformation¹¹ implemented in a realistic way.⁴ This is in contrast to the fact that the standard LDA + DMFT based on solving the Anderson model, which was used, e.g., in Ref. 12 for δ -Pu, typically can reach temperatures down to $O(100)$ K if the core impurity problem is to be exactly solved by the QMC method. Here some basis-cutoff schemes have been implemented¹³ to reduce the computational cost.

One of the reasons plutonium compounds have been interesting and difficult to address is that they reside on the border of itinerancy and localization of $5f$ electrons among actinides.^{14,15} At least for Pu chalcogenides and pnictides, experimental evidence for localized $5f$ electrons was revealed,¹⁶ and a recent theoretical work¹⁷ agrees with that, so these can be benchmark cases for the realistic KLM simulations. For Pu-115's it has been known that the Curie law persists down to the superconducting temperature for PuCoGa₅ (Ref. 1), which supports the presence of localized $5f$ electrons, but some attention must be reserved for a possible sample dependence: radiative Pu decays into U, which can introduce magnetic impurities. It is thus controversial whether the Curie-Weiss law is intrinsic or not.¹⁸ Analyses of experiments point to $n_f = 5.03$ for δ -Pu,¹⁴ which we believe is sufficient for the KLM to work. The valence deduced from the calculations shows a much larger spread (between 4¹⁹ and 6²⁰) with the values of 5.2 for δ -Pu (Ref. 21) and 5.26 for PuCoGa₅ (Ref. 22) from most accurate continuous-time (CT) QMC calculations.

Our realistic KLM framework for the above-mentioned Pu compounds consists of two steps: (i) LDA for delocalized s -, p -, and d -conduction electrons and the Hubbard-I approximation²³ for the self-energy of localized f electrons

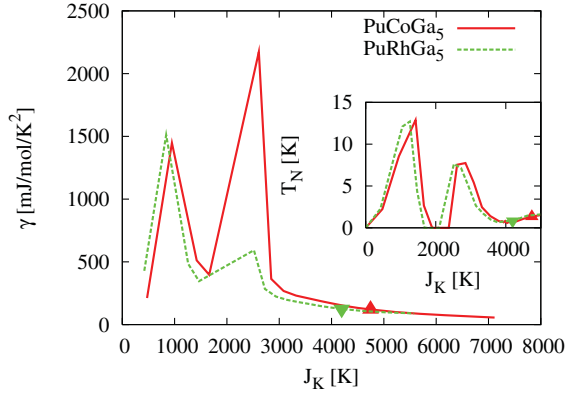


FIG. 1. (Color online) Summary of our results for Pu-115's on a realistic Doniach phase diagram. The realistic data point is indicated by the symbol on the line for each target material. The main panel shows the trend among Sommerfeld coefficients, and the inset shows the Néel temperatures.

gives us the partial densities of states and hybridization functions as prescribed by the LDA + DMFT framework.⁷ The data are summarized in Table I. It is clear that Pu-115's have much higher energy scales than the cerium ones.⁵ (ii) We solve the low-energy effective KLM Hamiltonian with dynamical mean-field theory,^{24,25} utilizing a state-of-the-art CT QMC solver^{13,26} for the lattice-embedded Kondo impurity problem.¹⁰ Thus our framework is self-consistent as far as the f electrons are well localized with the approximation that the charge fluctuations for f electrons are neglected. For the $5f$ orbitals of Pu, it is known that there is a big spin-orbit splitting of 1 eV and the five possibly localized electrons fill in the lower $j = 5/2$ multiplet up to leaving one localized hole.²⁷ Photoemission experiments show that the level of the localized hole is separated from the Fermi level by 1 eV, which is verified by our theoretical estimates. We neglect the crystal-field splittings, which are known to be small in Pu compounds in the local $5f$ level.

Solving an inverse problem to restore f electrons. Even if we eliminated f electrons and kept only f spins in our KLM, part of the information for the localized f electrons can be restored from the relation $\Sigma_c(i\omega_n) \equiv V^2/[i\omega_n - \epsilon_f - \Sigma_f(i\omega_n)]$, where Σ_c is our conduction-electron self-energy, $i\omega_n = (2n + 1)\pi T$ is the Matsubara frequency, $\epsilon_f = -1$ eV is the position of the impurity level, and Σ_f is the f -electron

TABLE I. Summary of LDA + Hubbard-I results for target materials. The unit of density of states, $N^{\text{tot}}(0)$ for all electrons and $N^f(0)$ for f electrons on the Fermi level, is states/Ry/cell.

Material	$N^{\text{tot}}(0)$	$N^f(0)$	$-\text{Tr}\Im\Delta(0)/\pi$ (eV)
PuCoGa ₅	34.33...	1.203...	0.705
PuRhGa ₅	33.03...	1.494...	0.912
δ -Pu	20.40...	2.781...	1.13
PuSe	17.30...	4.342...	0.619
PuTe	13.45...	0.7729...	0.360
PuAs	8.351...	0.6068...	0.255
PuSb	10.01...	0.2699...	0.193
PuBi	7.723...	0.2534...	0.133

self-energy, which we do not have explicitly in our KLM calculations. Provided that we reach the temperature for a given target material to be in a Fermi-liquid region concerning its f electrons, which is mostly the case for Pu compounds, the quasiparticle renormalization factors are well defined and are written as $z_x = [1 - \partial\Im\Sigma_x(i\omega_n)/\partial(i\omega_n)]^{-1}$, with $x = c$ and f for conduction electrons and f electrons, respectively. Here the derivative is taken at $i\omega_n = 0$. We get from the above definition of Σ_c the following inversion relation: $z_f = [|\Sigma_c(0)|^2/V^2]z_c/(1 - z_c)$. Because z are written in terms of the derivative of the corresponding self-energy at the lowest frequency, our effective low-energy description based on KLM enables a good solution of this inverse problem as far as z_f is concerned. The Sommerfeld coefficient $\gamma = (1/3)\pi^2 N_{\text{eff}}(0)$, where $N_{\text{eff}}(0)$ is the effective total density of states (DOS) on the Fermi level, can be estimated by $N_{\text{eff}}(0) = N_c(0)/z_c + N_f(0)/z_f$, where $N_c(0)$ is the DOS of s -, p -, and d -conduction electrons and $N_f(0)$ is that of the localized f electrons in our LDA + Hubbard-I calculations. With a given KLM, we extract z_c from Σ_c obtained after DMFT, invert it to z_f , and get the Sommerfeld coefficient γ with the above formula. In this way we can restore an analog of the Doniach phase diagram for γ , as shown in Fig. 1 for Pu-115's. The results on the realistic data point for each target material are summarized in Table II together with the experimental data taken from the literature. Our prediction follows the experimental trend among γ semiquantitatively. We note that γ is sensitive to the estimate of the realistic point of J_K , especially around QCP's, considering the sharp peak structure as seen in Fig. 1 for the plot of γ vs J_K . So the overall trend among materials is the most important result.

Magnetism and quasiparticle renormalizations. The results for magnetism are schematically summarized in Fig. 2 for all target materials in the format of a rescaled Doniach phase diagram. It illustrates how we understand the results in the inset of Fig. 1 for Pu-115's.

TABLE II. Summary of our data obtained with realistic Kondo lattice simulations and our prediction for γ based on them. The unit of γ is mJ/mol/K². Experimentally known results are taken from the literature.

Material	z_f	z_c	Our γ	Experimental γ
PuCoGa ₅	0.0403	0.0496	120	80 ^a –116 ^b
PuRhGa ₅	0.0367	0.0462	130	50 ^a –80 ^c
δ -Pu	0.0625	0.0738	49	50–64 ^d
PuSe	0.0480	0.0232	110	90 ^e
PuTe	0.00883	0.0313	85	30 ^f –60 ^e
PuAs	0.0588	0.00456	295	
PuSb	0.0231	0.0168	102	6 ^b –20 ^g
PuBi	0.00202	0.0965	35	

^aReference 31.

^bReference 32.

^cReference 33.

^dReference 34.

^eReference 30.

^fReference 35.

^gReference 36.

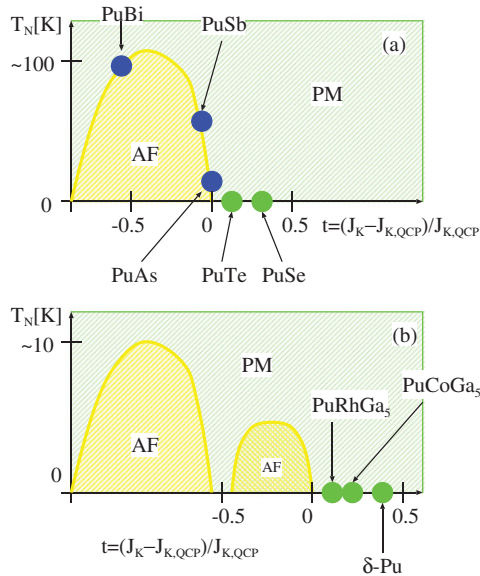


FIG. 2. (Color online) Schematic summary of our magnetic phase diagrams for Pu compounds plotted on the (t, T_N) plane, where $t \equiv (J_K - J_{K,QCP})/J_{K,QCP}$ being the first QCP in (a) and the third QCP in (b).

A striking multidome structure shows up together with multiple QCP's for materials with strong Kondo coupling. We find that Pu-115's are located in a region where the antiferromagnetic long-range order is suppressed, possibly near a hidden or pseudo-QCP, within some numerical noise at the lowest reachable temperatures at present. Inspecting the distribution of materials around the QCP's in Fig. 2, we have pnictides on the left-hand side and chalcogenides on the right-hand side of the antiferromagnetic QCP. This is consistent with what has been known experimentally; that is, pnictides, such as PuAs, PuSb,²⁸ and PuBi,²⁹ are magnets and chalcogenides, such as PuSe and PuTe, are paramagnets.³⁰ The actual magnetism is strongly spatially anisotropic,^{15,29} and its treatment is unfortunately beyond the level of single-site DMFT description. For now, we will leave the issue of ordering wave vectors for future presentations and focus on the trends across target materials spanning between magnetism and HF behavior. The characteristic energy scales of Kondo screening and magnetic ordering have been captured by fully incorporating the frequency dependence of the hybridization.

The multidome structure together with multiple QCP's shown in Fig. 1 for Pu-115's can be understood in terms of the strong-coupling nature of the Kondo lattice⁹ based on the growth of the characteristic Kondo energy scale T_K with respect to J_K , as shown in Fig. 3(a), which is obtained from our local susceptibility data. Simple perturbative arguments also prompt two crossover points between competing energy scales of the KLM:⁸ $T_{RKKY} \sim J_K^2 \rho$ and $T_K \sim \exp[-1/(J_K \rho)]/\rho$, where the latter can saturate at some point with respect to large J_K , while the former keeps on growing. Here ρ is the characteristic DOS of conduction electrons.

We demonstrate our predictive power regarding T_K also for the case of δ -Pu, where we get $T_K \sim 10^3$ [K] from our local susceptibility data, which is seen to be close to the previous results, $T_K \sim 700$ [K] in Ref. 21. We note that the Kondo

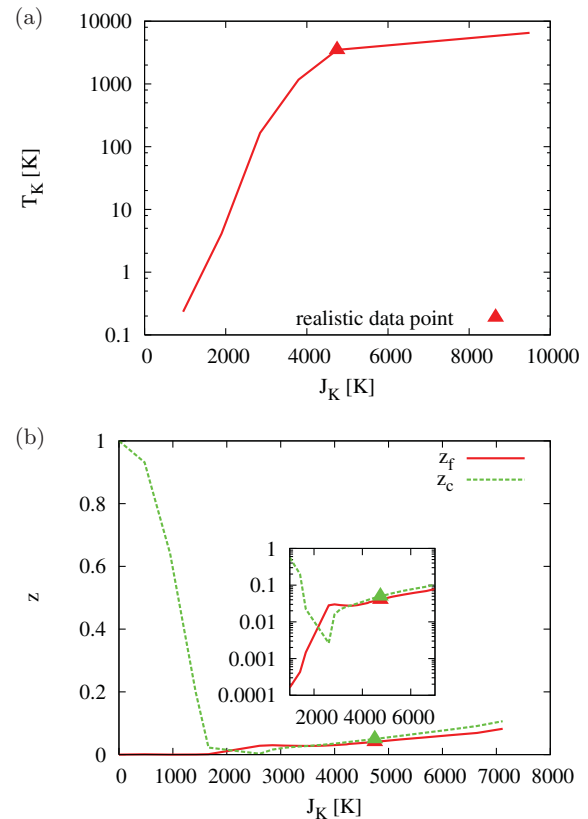


FIG. 3. (Color online) Analog of Doniach phase diagram for (a) Kondo temperature and (b) quasiparticle renormalization factors for PuCoGa₅. The inset in (b) is a zoom-in picture around the first QCP with the vertical axis plotted in logarithm scale.

screening energy scale is approaching a comparative scale to the characteristic bandwidth, or the kinetic energy of the conduction electrons, which is $O(1)$ eV. Such a situation has been discussed in the literature^{9,37} in the context of models, which is now found to be realized in plutonium heavy-fermion materials.

The behavior of quasiparticle renormalization factors z_x ($x = c$ or f) as shown in Fig. 3(b) further gives the physical picture: starting from $J_K = 0$, where there are free conduction electrons and completely localized f electrons with $(z_c, z_f) = (1, 0)$, the former gradually gets renormalized toward the first QCP, and f electrons gets “delocalized” in the sense that they start to take part in Fermi surface (FS).^{38,39} Passing the first QCP, heavy quasiparticles composed both of conduction electrons and f electrons evolve together after z_c has shown a dip around the first QCP, letting f spins show up again with the underscreening effects that correspond to the slightly elevated z_c . Thus after the revival of magnetism the same thing can happen again and could repeat itself, with redefined, much smaller energy scales every time, all the way to the $J_K \rightarrow \infty$ limit, which is consistent with the phase diagram obtained in Ref. 9.

This strong-coupling KLM scenario for Pu compounds can, in principle, be checked by de Haas–van Alphen experiments, which would measure the size of the FS to see if it counts the number of “localized” f electrons. The ferromagnetic phase of PuAs should be the one with the “large” FS including

the spins of localized $5f$ electrons. This phase would be in contrast to the typical magnetic phases in HF compounds with the “small” FS, which is located in the weak-coupling region. Following the method of Ref. 39, we can track the evolution of large FS for representative Pu compounds obtained from $-\Re \Sigma_c(i\omega_n)|_{i\omega_n=0}$, and we find that PuAs shows a remarkable evolution of large FS, which should be compared with experiments to see if the strong-coupling KLM picture can hold.

Conclusions. We have found that multiple QCP’s show up for plutonium-based materials that have stronger Kondo couplings than their cerium counterparts. Our methodology captures the quasiparticle renormalization factor and the

characteristic energy scale correctly. The striking multidome feature of the Doniach phase diagrams for Pu-115’s and δ -Pu as well as the magnetic and HF behavior among Pu pnictides and chalcogenides is understood on the basis of the strong-coupling limit of KLM. This picture can be verified by looking at the size of the Fermi surface for PuAs.

Acknowledgments. The authors thank E. D. Bauer, A. V. Chubukov, P. Coleman, N. J. Curro, R. Dong, M. J. Han, K. Haule, K. Kim, G. Kotliar, H. Shishido, Y.-F. Yang, and C.-H. Yee for discussions. The present numerical calculations have been done on “Chinook” at the Pacific Northwest National Laboratory. This work was supported by DOE NEUP Contract No. 00088708.

-
- ¹J. L. Sarrao *et al.*, *Nature (London)* **420**, 297 (2002).
²N. J. Curro *et al.*, *Nature (London)* **434**, 622 (2005).
³R. Flint, M. Dzero, and P. Coleman, *Nat. Phys.* **4**, 643 (2008).
⁴M. Matsumoto, M. J. Han, J. Otsuki, and S. Y. Savrasov, *Phys. Rev. Lett.* **103**, 096403 (2009).
⁵M. Matsumoto, M. J. Han, J. Otsuki, and S. Y. Savrasov, *Phys. Rev. B* **82**, 180515(R) (2010).
⁶For a review, see S. Sachdev, *Quantum Phase Transitions* (Cambridge University Press, New York, 1999).
⁷For a review, see G. Kotliar, S. Y. Savrasov, K. Haule, V. S. Oudovenko, O. Parcollet, and C. A. Marianetti, *Rev. Mod. Phys.* **78**, 865 (2006).
⁸S. Doniach, *Physica (Amsterdam)* **91B+C**, 231 (1977).
⁹C. Lacroix, *Solid State Commun.* **54**, 991 (1985).
¹⁰J. Otsuki, H. Kusunose, P. Werner, and Y. Kuramoto, *J. Phys. Soc. Jpn.* **76**, 114707 (2007).
¹¹J. R. Schrieffer and P. A. Wolff, *Phys. Rev.* **149**, 491 (1966).
¹²C. A. Marianetti, K. Haule, G. Kotliar, and M. J. Fluss, *Phys. Rev. Lett.* **101**, 056403 (2008).
¹³K. Haule, *Phys. Rev. B* **75**, 155113 (2007).
¹⁴For a review, see K. T. Moore and G. van der Laan, *Rev. Mod. Phys.* **81**, 235 (2009).
¹⁵For a review, see P. Santini, R. Lémanski, and P. Erdős, *Adv. Phys.* **48**, 537 (1999).
¹⁶T. Gouder, F. Wastin, J. Rebizant, and L. Havela, *Phys. Rev. Lett.* **84**, 3378 (2000).
¹⁷C. H. Yee, G. Kotliar, and K. Haule, *Phys. Rev. B* **81**, 035105 (2010).
¹⁸A. Hiess, A. Stunault, E. Colineau, J. Rebizant, F. Wastin, R. Caciuffo, and G. H. Lander, *Phys. Rev. Lett.* **100**, 076403 (2008).
¹⁹O. Eriksson, J. D. Becker, A. V. Balatsky, and J. M. Wills, *J. Alloys Compd.* **287**, 1 (1999).
²⁰L. Havela *et al.*, *J. Alloys Compd.* **444-445**, 88 (2007).
²¹J. H. Shim, K. Haule, and G. Kotliar, *Nature (London)* **446**, 513 (2007).
²²M. E. Pezzoli, K. Haule, and G. Kotliar, *Phys. Rev. Lett.* **106**, 016403 (2011).
²³J. Hubbard, *Proc. R. Soc. London, Ser. A* **276**, 238 (1963); **277**, 237 (1964); **281**, 401 (1964).
²⁴A. Georges, G. Kotliar, W. Krauth, and M. J. Rozenberg, *Rev. Mod. Phys.* **68**, 13 (1996).
²⁵J. Otsuki, H. Kusunose, and Y. Kuramoto, *J. Phys. Soc. Jpn.* **78**, 014702 (2009).
²⁶P. Werner, A. Comanac, L. de’ Medici, M. Troyer, and A. J. Millis, *Phys. Rev. Lett.* **97**, 076405 (2006).
²⁷The analogy between cerium and plutonium compounds was discussed earlier by B. R. Cooper, P. Thayamballi, J. C. Spirlet, W. Müller, and O. Vogt, *Phys. Rev. Lett.* **51**, 2418 (1983). Also, a similar model has been discussed recently by C. D. Batista, J. E. Gubernatis, T. Durakiewicz, and J. J. Joyce, *Phys. Rev. Lett.* **101**, 016403 (2008).
²⁸P. Bulet, S. Quezel, J. Rossat-Mignod, J. C. Spirlet, J. Rebizant, W. Muller, and O. Vogt, *Phys. Rev. B* **30**, 6660 (1984).
²⁹K. Mattenberger, O. Vogt, J. C. Spirlet, and J. Rebizant, *J. Magn. Magn. Mater.* **54-57**, 539 (1986).
³⁰J. M. Fournier *et al.*, *Phys. B* **163**, 493 (1990).
³¹J. D. Thompson, N. J. Curro, T. Park, E. D. Bauer, and J. L. Sarrao, *J. Alloys Compd.* **444-445**, 19 (2007).
³²P. Javorský, F. Wastin, E. Colineau, J. Rebizant, P. Boulet, and G. Stewart, *J. Nucl. Mater.* **344**, 50 (2005).
³³J. L. Sarrao and J. D. Thompson, *J. Phys. Soc. Jpn.* **76**, 051013 (2007).
³⁴J. C. Lashley, J. Singleton, A. Migliori, J. B. Betts, R. A. Fisher, J. L. Smith, and R. J. McQueeney, *Phys. Rev. Lett.* **91**, 205901 (2003).
³⁵G. R. Stewart, R. G. Haire, J. C. Spirlet, and J. Rebizant, *J. Alloys Compd.* **177**, 167 (1991).
³⁶R. O. A. Hall, A. J. Jeffery, and M. J. Mortimer, *J. Less Common Met.* **121**, 181 (1986).
³⁷M. Sigrist, H. Tsunetsugu, K. Ueda, and T. M. Rice, *Phys. Rev. B* **46**, 13838 (1992).
³⁸R. M. Martin, *Phys. Rev. Lett.* **48**, 362 (1982).
³⁹J. Otsuki, H. Kusunose, and Y. Kuramoto, *Phys. Rev. Lett.* **102**, 017202 (2009).